DEVELOPMENT OF FLEXIBLE BARRIER AND EVALUATION OF ITS EFFECTIVENESS

Yoshitsugu KIMURA[1]*, Hiroyuki UMEZAWA[1], Yoshiiku MUSASHI[2], and Takahisa MIZUYAMA[3]

[1] Toa Grout Kogyo Co., Ltd. (2-10-3 Yotsuya, Shinjuku, Tokyo 1600004, Japan)
[2] Yachiyo Engineering Co., Ltd. (2-18-12 Nishiochiai, Shinjuku, Tokyo 1618575, Japan)
[3] Kyoto University (Kitashirakawaoiwakecho, Sakyouku, Kyoto 6068502, Japan)
*Corresponding author. E-mail: yoshitugu.kimura@toa-g.co.jp

Since the enactment of the Law related to Promotion of Measures for Sediment-related Disaster Area etc. due to Sediment-related Disaster[*Japan Society of Erosion Control Engineering*,2004], numerical conditions for designing structures for catching collapsed soil in steep slope failure prevention areas have been clarified. This improvement is meant to provide structures for catching collapsed soil with greater resistance to its impact force and the earth pressure, and maintain the capacity of these structures to retain the required volume of collapsed soil. Concrete retaining walls have been widely used as structures for it, but since the walls that serve this purpose are rigid, large structures and a wide area are required. As an alternative to conventional structures, we have developed a new type of structure for catching collapsed soil for slope failure prevention that is compact and flexible (hereinafter "flexible barrier"). The performance of the flexible barrier are achieved by tolerating large deformation, thus mitigating the impact force of collapsed soil.

Fig. 1 Flexible barrier for catching collapsed soil

Fig. 2 Retaining wall for catching collapsed soil

Key words: full-scale test, energy-absorbing elements, DEM

1. HISTORY OF DEVELOPMENT

1.1 Performance Requirements of Slope Failure Prevention Works

Following the enactment of the Law related to Promotion of Measures for Sediment-related Disaster Area etc. due to Sediment-related Disaster [*Notification of the Ministry of Land, Infrastructure, Transport and Tourism No. 332*, 2001], the calculation method of the amount of collapsed soil in addition to the impact force of collapsed soil and the deposit pressure necessary to designate sediment disaster special alert areas has been specified.

This then requires compliance with the following conditions when slope failure prevention works are designed in steep slope failure prevention areas:

(1) Impact force working on the structure (F)

$F=\alpha\cdot F_{sm}$

where

$$F_{sm}=\rho_m g h_{sm}\left[\left\{\frac{b_u}{a}\left(1-\exp\left(-2aH/h_{sm}\sin\theta_u\right)\right)\cos^2(\theta_u-\theta_d)\right\}\exp\left(-2aX/h_{sm}\right)+\frac{b_d}{a}\left(1-\exp\left(-2aX/h_{sm}\right)\right)\right]$$

$$a=\frac{2}{(\sigma-1)\cdot C+1}\cdot f_b$$

$$_u=b\ \cos\theta_u\left\{\tan\theta_u-\frac{\sigma(-1)C}{\sigma(-1)C+1}\cdot\tan\phi\right\}$$

$$_d=b\ \cos\theta_d\left\{\tan\theta_d-\frac{\sigma(-1)C}{\sigma(-1)C+1}\cdot\tan\phi\right\}$$

where

F: Impact force acting on the barrier
F_{sm}: Flowing sediment force
α: Empirical factor of impact force
θ: Slope Inclination
H: Slope height
X: Flat space behind barrier
h_{sm}: Thickness of flowing sediment
C, σ, ϕ: Constants of sediment

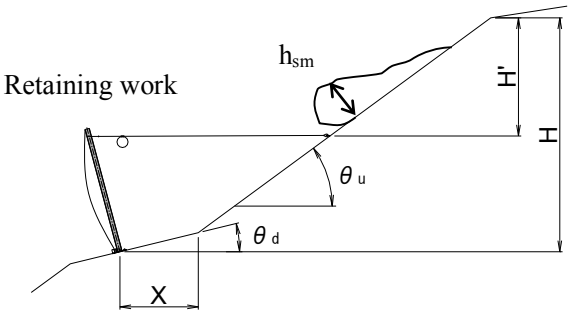

Fig. 3 Definition of key dimensions used in the calculation

(2)Earth pressure working on the structure (F_{sa})

$$F_{sa}=\frac{\gamma\cdot h\cdot\cos^2\phi}{\cos\delta\left(1+\sqrt{\frac{\sin(\phi+\delta)\cdot\sin\phi}{\cos\delta}}\right)^2}$$

Where

F_{sa}: Earth pressure at rest
h: Height of barrier
ϕ: Internal friction angle of sediment

(3) Amount of collapsed soil
If it is difficult to turn to local geological surveys or failure records, the value of 90% of the amount of collapsed soil, contained in the landslide failure disaster data nationwide, classified by slope height, should be used as a reference [*Japan Flexible Barrier Association*, 2013].

Table 1 Amount and width of collapsed soil

Slope height (m)	Amount of collapsed soil V (90% value) (m^3)	Failure width W (m)	Unit amount of collapsed soil V/W (m^3/m)
$5 \leq H < 10$	40	14	2.9
. . .	. . .	. . .	. . .
$50 \leq H$	500	32	15.6

1.2 Current Status of Concrete Retaining Walls

For concrete retaining walls that have been conventionally constructed as slope prevention works, many of them are designed only for back-side earth pressure and therefore have poor resistance to impact force. Therefore, they need to be very large in structural body in order to ensure the predetermined catch capacity.

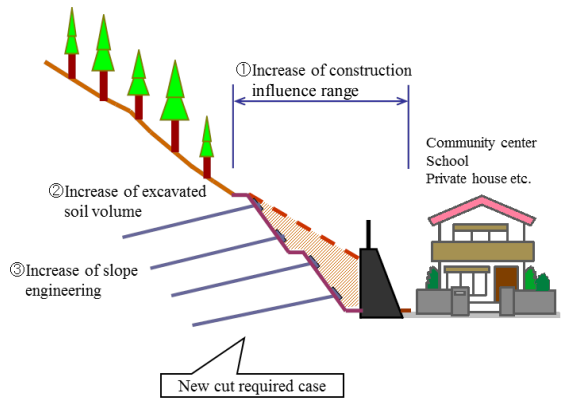

Fig. 4 Plan of construction of retaining walls

Eventually, where buildings are located close to slopes, cases occurred where the slopes had to be cut to plan construction of retaining walls (see Fig. 4).

In addition, since facilities of rigid construction like retaining walls are poor in resistance to impact, some retaining walls are reported to have been overturned or suffered partial damage by collapsed soil.

1.3 Development of Flexible Barrier

A high-energy rock fall protection fence (hereinafter "high-energy fence") was used as a candidate for development of a new type of slope failure prevention works that can solve the following conditions, and the development work was started:

(1) The new barrier shall have a structure that allows easy construction on the upper part of the slope in confined spaces where it is difficult to install the conventional type of slope failure prevention works.
(2) It shall be capable of being installed on the upper part of the slope of the existing slope failure prevention works and compensating for the performance deficiency of the existing works.
(3) It shall satisfy the three conditions required of the earlier-mentioned slope failure prevention works.

The high-energy fence was chosen as the basic model because it has been installed at many sites in Japan and characteristically tolerates large deformation to absorb large kinetic energy. It is therefore considered to be sufficiently resistant to the impact of collapsed soil.

However, the performance-verification-type design criteria specify the member constitution of high-energy fences depending on the level of kinetic energy of rock fall, with implementation of a full-scale test as the prerequisite.

Therefore, it is now required to verify its resistance to the catch capacity of collapsed soil in addition to the capability of resisting the forces of impact and earth pressure.

1.4 Basic Structure of Flexible Barrier

The authors adopted a policy of developing a flexible barrier as a modified version of the high-energy fence. Utilizing the advantages of the high-energy fence, it is envisaged that the flexible barrier be composed of ring nets braided with high-strength hard steel wires, wire ropes, the brake rings of the energy absorbers being attached to the wire ropes, posts and anchors.

Of these, the ring net and brake ring are the members that accept large deformation and greatly contribute to energy absorption. The status of deformation when the works receive impact is shown in Fig. 5.

It was necessary to select members from the following group popularly used for high-energy fences in order to maintain versatility and economy.

(1) Ring net
5 to 19 turns of high tensile steel wires (breaking strength of 1,770 N/mm^2)
(2) Wire rope
ϕ16 to ϕ22, GEOBINEX ϕ22
(3) Brake ring
Six types depending on the wire rope diameter
(4) Post
H steel: 175 to 250 mm

Fig. 5 Status of deformation when the works receive impact

2. ESTABLISHMENT OF THE DESIGN METHOD

2.1 Design Method based on Equilibrium of Force

While dynamic analysis has been mainly used for structures that tolerate large deformation in general, we decided to use the member design procedure based on the allowable stress method by considering the following conditions and assuming the equilibration of force in fence deformation:

(1) Since there are a variety of slope shapes and failure shapes that are to be considered in design, it is essential that the appropriate design can be relatively easily conducted to realize application to many locations.
(2) It is also essential that appropriate post intervals and post heights can be set depending on the topographical condition of the slope and the necessary catch capacity.
(3) The appropriate design method shall involve calculation of the force that will work on each member based on the impact force of collapsed soil and the deposit pressure and selection of appropriate members from the earlier-mentioned options.

The concept of equilibrium of force against the action of impact force is illustrated in Fig. 6.

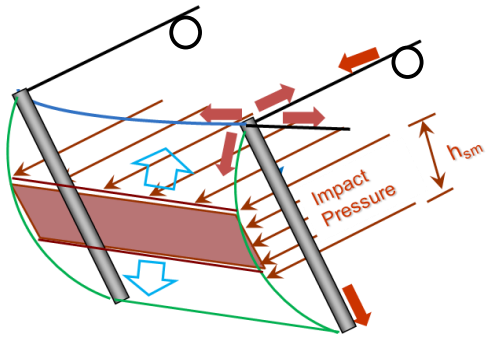

Fig. 6 Concept of equilibrium of force against the action of impact force

This method allowed us to compare the force working on members under the action of impact force and under the action of deposit pressure and to relatively easily select appropriate members.

Safety factors for members were appropriately determined in the design. To be specific, the safety factors generally used for wire ropes and posts when they are under the impact force were used. The problem left unsettled was the safety factor for the ring net, which is a member uniquely developed by us.

The ring net would not entirely deform evenly when the impact force acted on it; deformation occurs differently depending on the location of the ring net as the transmission direction of force and the deformation shape differ from place to place. It was therefore necessary to direct deformation in the direction that can ensure safety of the ring net in terms of design.

The results of unit member tensile testing and the case examples of high-energy fences having caught sediments were studied, and a value of 7.0 was chosen for the safety factor (Sf) of the ring net.

In addition, a full-scale model experiment was

conducted to check the safety of the fence structure constructed to this design method.

2.2 Design Method of the Debris Catch Capacity

The amount of collapsed soil is determined by the mode of slope failure or the height of slope as earlier mentioned.

Since the flexible barrier tolerates large deformation, it needs to maintain the prescribed catch capacity after being deformed.

Usually after the barrier has caught debris, the sag of the post rope increases to eventually lower the height of the barrier, an important factor that makes the barrier catch debris effectively.

However, the deformation of the ring net can increase catch capacity (see Fig. 7).

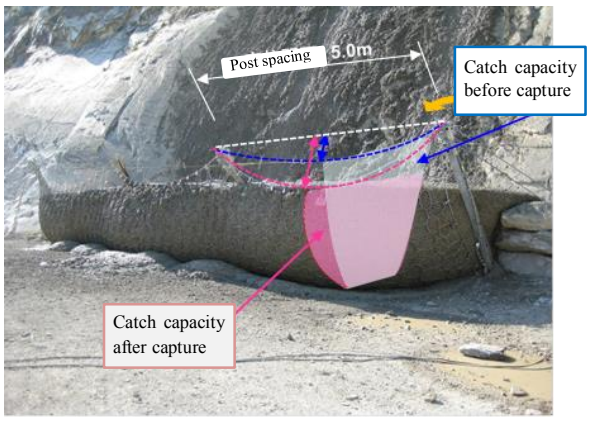

Fig. 7 Concept of equilibrium of force against the action of impact force

These deformation shapes were then examined in the full-scale test, and an equation uniquely developed to determine the barrier height was established together with other factors that determine the catch capacity as shown below:

$h = f\,(Xs, X, \theta)$

h: post height Xs: post distance X: width of flat space behind barrier θ: slope inclination

Multivariable analysis with the above three factors changed in a few patterns was conducted in the range roughly confirmed by the full-scale test, and the equation was established that allows determination of the barrier height that can ensure the prescribed catch capacity both before and after deformation of the barrier.

3. PERFORMANCE VERIFICATION WITH FULL-SCALE TEST

Full-scale tests were conducted several times to confirm the safety of the design method and deformation at two different topographical conditions. The test's conditions, shown in Figs. 8 and 9 were chosen to represent steep slope failure hazard area in Japan [*SABO & Land slide Technical Center*, 2011]. The debris material was a mixture of gravel, silt and clay. The debris was stored in a container at the top of the slope. During the test, the debris was released and allowed to run down towards the test barrier at the toe of the slope by opening the release gate. Some key measurements such as acting force on wire ropes, the height of debris, the speed of debris, the pressure of debris, deformation of brake ring and ring net, the degree of rotation of posts, etc. were taken. Some typical results for the tests that had successfully captured the debris without breakage of key structural components and excessive deformation are summarized below.

Table 2 Different topographical conditions and results of full-scale tests

	Test site A	Test site B
Impacting width	15.0 m	8.0 m
Post height	3.5 m	3.5 m
Maximum impact pressure acted on net (calculated or measured)	103 kN/m^2	155 kN/m^2
Maximum deformation of net from the bottom of post	2.3 m	3.2 m

Fig. 8 Test site A in St.Leonard, Switzerland

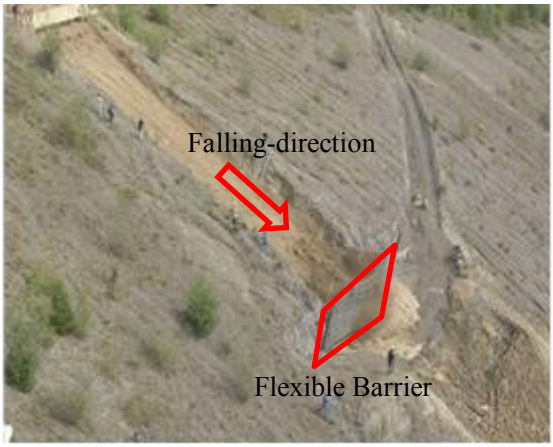

Fig. 9 Test site B in Feltheim, Switzerland

The maximum impact pressure acted on net 155 kN/m^2 at Test site B is calculated numerical value from measured one, 170 kN/m^2 by earth pressure gage attached on upper side of the slope.

In practice, we should always keep the facility to be protected at a distance more than the post height away from the flexible barrier itself.

4. COMPARISON BETWEEN RETAINING WALL AND FLEXIBLE BARRIER

4.1 Modeling by Distinct Element Method (DEM)

Simulation by the distinct element method (DEM) [*Musashi, Y., et al.*, 2011] was conducted to confirm the differences in the behavior of, or the acting force upon capture of collapsed soil between the retaining wall, the structure conventionally used for steep slope failure prevention works, and the flexible barrier.

DEM is a method that expresses a force working among elements with springs and dashpots, as shown in Fig. 10 The flexible barrier is modeled as in Fig. 11 to enable DEM to handle behaviors as complicated as those of the flexible barrier.

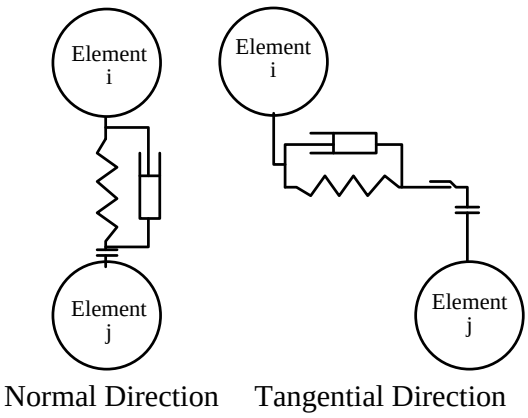

Fig. 10 Concept of the distinct element method (DEM)

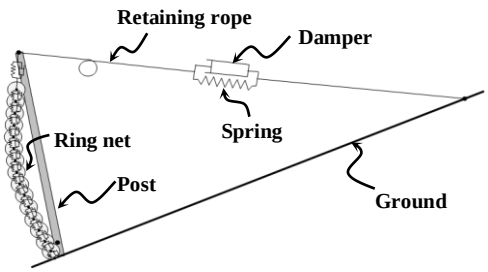

Fig. 11 Modeling of the flexible barrier

4.2 Reproduction Calculation on Case of Retaining Wall Failure

Reproduction calculation was conducted for a case of a retaining wall overturned by a slope failure that occurred in Kirishima City, Kagoshima Prefecture, in order to confirm the validity of DEM analysis of the process of collapsed soil capture by the retaining wall.

In this case example, a slope, 70 m in height and 35° in slope gradient, collapsed with a failure height and width of 46 m and 30 m respectively, and the gravity retaining wall, 4 m in elevation and 28 m in width in the transverse direction, at the lower end of the slope was eventually slid and overturned.

The reproduction calculation conditions are shown in Table 3, while the calculation results are shown in Fig. 12. It is reported that the retaining wall moved by about 5 m. Although the reproduction calculation result produced a relatively small movement distance of the retaining wall, the sliding and overturning conditions were reproduced.

Table 3 Analysis conditions of reproduction calculation for the retaining wall damage case

Item			Unit	Value	Remarks
Collapsed soil	Failure width		[m]	30	
	Element radius		[mm]	75	
	Element density		[t/m]	2.65	
	No. of elements		[qt]	4,268	50% mixed with particles each composed of two tied elements
	Spring coefficient	Normal direction	[kN/m^3]	100000	
		Tangential direction	[kN/m^3]	35700	
	Coefficient of restitution			0.2	
	Friction angle		[degree]	35.0	Applied to the area between the ground and the retaining wall
Retaining wall	Retaining wall height		[m]	4.0	
	Retaining wall width		[m]	28	
	Spring coefficient	Normal direction	[kN/m^3]	100000	
		Tangential direction	[kN/m^3]	41700	
	Coefficient of restitution			0.2	
	Element density		[t/m]	2.3	Density of ordinary concrete

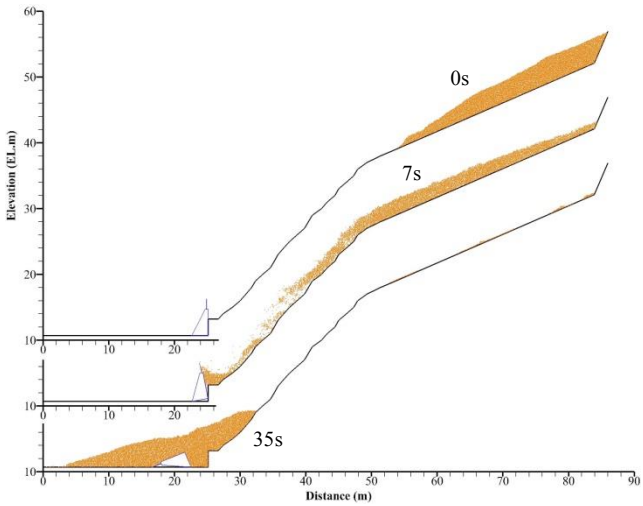

Fig. 12 Result of reproduction calculation of the retaining wall damage case

4.3 Reproduction Calculation of the Full-scale Flexible Barrier Test

Reproduction calculation was conducted for a full-scale test in order to verify the validity of the DEM analysis of the process of the flexible barrier's capture of collapsed soil. The structure of flexible barrier was equivalent to that used in full-scale test. Spring conditions including those for the ring net and retaining rope were determined, as shown in Table 4, so that the conditions would produce good reproducibility of the full-scale test conducted at an experiment field in Feltheim, Switzerland, in September 2010.

In this experiment, a flow channel measuring 8 m in width and 30° in gradient was constructed in the slope, and sediments were discharged down the channel twice. In the first discharge, sediments in the volume of 50 m^3 were released, but got deposited halfway down the channel, and 10 m^3 were caught by the flexible barrier. In the second discharge, all of the sediments, or 50 m^3, were caught by the barrier.

Since it is difficult for reproduction calculation to reproduce the deposition of the sediments halfway down the channel, 10 m^3 were released in the first discharge, and 50 m^3 in the second discharge.

Fig. 13 shows the collapsed soil and the change in the shape of the flexible barrier. In the experiment, the ring net was deformed in the downstream direction by about 1 m in the first discharge and about 2 m in the second discharge. A good agreement of the shape is indicated in Fig. 13.

Fig. 14 plots changes in tensile force of the retaining rope. The analysis results indicate that the sediment moved faster and arrived earlier than in the experiment result. The peak values of the tensile force upon impact mostly agreed.

Table 4 Analysis conditions of reproduction calculation for the full-scale test of the flexible barrier

Item			Unit	Value	Remarks
Collapsed soil	Failure width		[m]	8	
	Element radius		[mm]	25	
	Element density		[t/m]	2.11	The total weight of the elements and the total weight of test specimens were equally determined.
	No. of elements		[qt]	2,848	50% mixed with particles each composed of two tied elements
	Spring coefficient	Normal direction	[kN/m³]	100000	
		Tangential direction	[kN/m³]	35700	
	Coefficient of restitution			0.2	
	Friction angle		[degree]	35.0	
Flexible barrier	Installation width		[m]	15	
	Fence height		[m]	3.5	
Ring net	Element radius		[mm]	50	
	Element density		[t/m]	0.05632	Determined to make the total weight of the ring net equal
	Spring coefficient		[kN/m]	20	Determined to produce good reproducibility
	Coefficient of viscosity		[kN/(m/s)]	0.49	
Retaining rope	Spring coefficient		[kN/m]	2500	
	Coefficient of viscosity		[kN/(m/s)]	982.5	

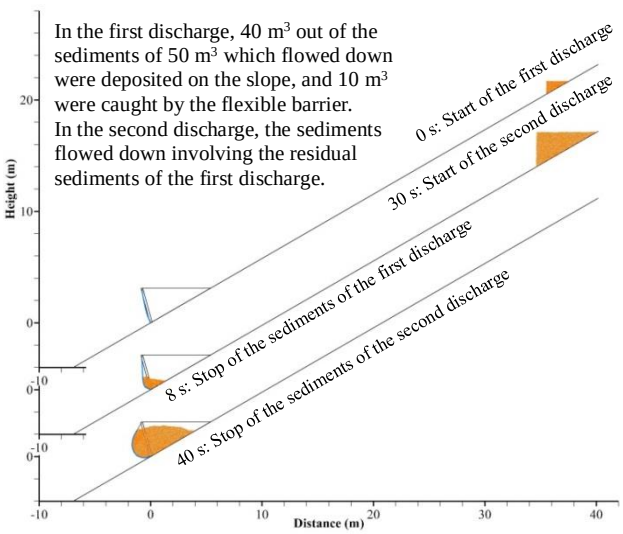

Fig. 13 Results of reproduction calculation for the full-scale test of the flexible barrier

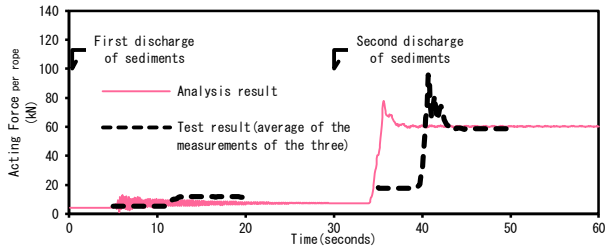

Fig. 14 Comparison of the retaining rope load ascertained in the experiment results and analysis results

4.4 Simulation with Failure Mode Changed

As shown in Fig. 15, Case 1, in which the impact force (force by movement) as per the Notification Equation is 100 kN/m^2, and Case 2, in which the impact force becomes 150 kN/m^2, are taken as the basic conditions of the failure specifications, and the amount of collapsed soil, gradient, failure height, and failure depth were changed in the analysis.

The specifications of the flexible barrier and retaining wall were determined so that the design conditions relative to the collapsed soil in Fig. 15 are each satisfied, as shown in Fig. 16 and Fig. 17, respectively. The number of retaining rope was increased in order to adopt to each impacting force. Furthermore, the acting force to flexible barrier related to post distance is converted as the force per unit length.

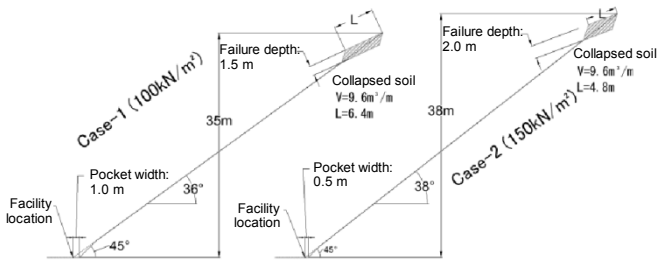

Fig. 15 Conditions for topography and collapsed soil

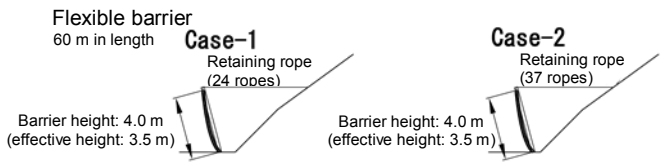

Fig. 16 Specifications of the flexible barrier

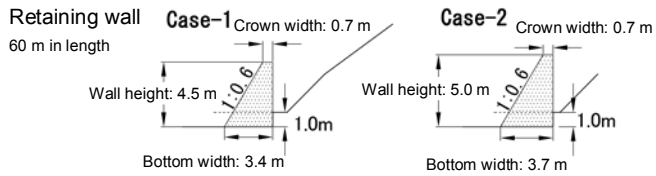

Fig. 17 Specifications of the retaining wall

As shown in Fig. 18, when the force the net receives from the collapsed soil is evaluated in terms of total acting forces, the weight of the sediment put on the net is added. Since it does not affect safety, both the flexible barrier and the retaining barrier were evaluated in the horizontal force in the downward direction.

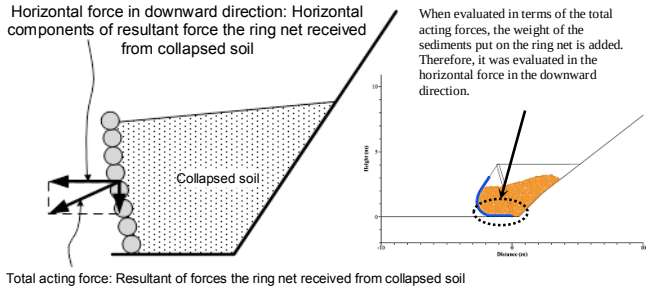

Fig. 18 Conceptual diagram of acting force

As shown in Fig. 19, the acting force by the deposit sediments, F_{dep}, is calculated from the average acting force in 20 s to 30 s upon the time of calculation completion, the maximum acting force from the start to end of analysis is taken as F_{max}, and impact force F_{imp} is estimated from the difference between F_{max} and F_{dep}.

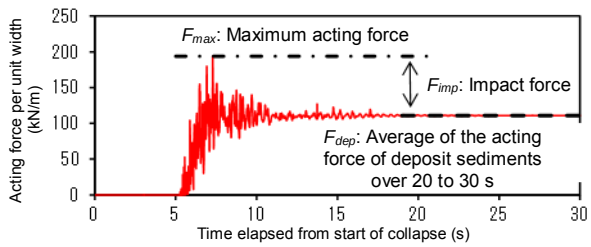

Fig. 19 Conceptual diagram of impact force evaluation

Acting forces given by the collapsed soil to the flexible barrier and retaining wall are explained based on the above concept and graphically expressed in Fig. 20.

The acting force exhibits a small increase as a result of increase in failure height. In the case of an increase in failure depth, the acting force tends to become smaller. This is probably because the greater the failure depth are, the more effective the down side collapsed soil become in preventing the starting movement of the upper side collapsed soil to slide downward.

In the case of an increase in the amount of collapsed soil and in slope gradient, the acting force tends to increase. The retaining wall started to slide down when the amount of collapsed soil exceeded 14.4 m^3/m in unit width and the slope gradient exceeded 45°. In these cases, since sliding reduced acting force, greater forces are assumed to work in cases where the

retaining wall does not slide down.

Comparing the acting forces between the flexible barrier and the retaining wall, both F_{dep} and F_{imp} are smaller for the flexible barrier, corresponding to about 60% of those for the retaining wall.

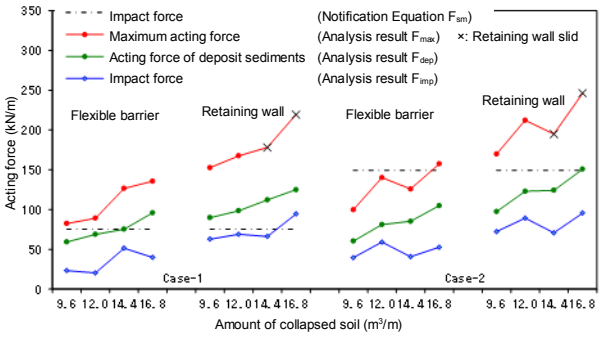

(a) When the amount of collapsed soil is changed

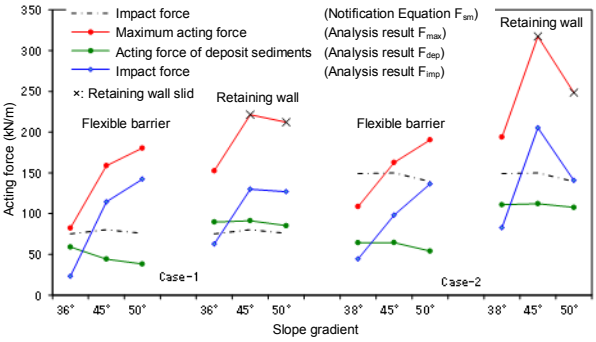

(b) When the slope gradient is changed

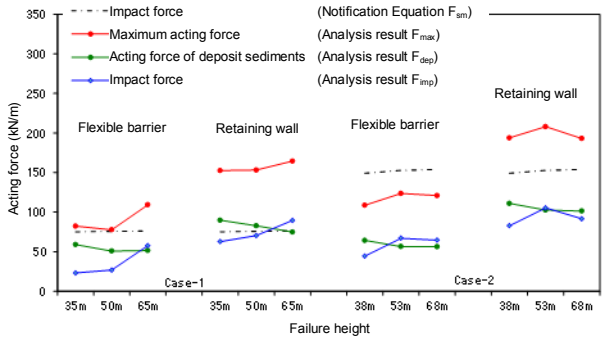

(c) When the failure height is changed

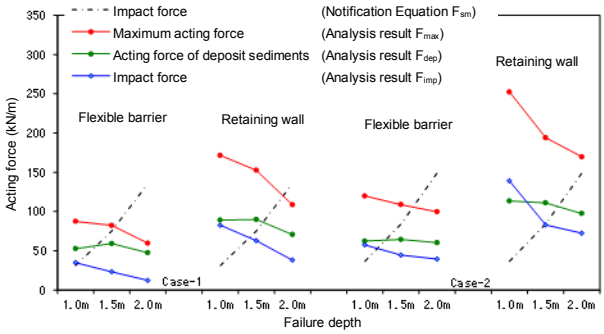

(d) When the failure depth is changed

Fig. 20 Changes in impact force when failure conditions are changed

It is speculated that the difference in acting force F_{dep} of deposit sediments is related to the expansion of the deposit area in the longitudinal direction by the deformation of the flexible barrier and the eventual decrease in the deposit depth. It is speculated that the difference in impact force F_{imp} is related to the effect of impact force absorption by the deformation of the flexible barrier upon impact.

Fig. 20 also includes the calculation results of impact forces as per the Notification Equation. Under fixed conditions (including a slope gradient of 45° or under), the calculation result of the impact force yielded by the simulation is smaller than that yielded by the Notification Equation.

5. INSTSLLATION CASE EXAMPLE AND DEBRIS CAPTURE CASE EXAMPLES

In Japan, so far there are about 40 sites where the flexible barrier has been successfully installed in steep slope failure hazard areas and road disaster prevention areas.

Figs. 21 and 22 show the sites of some of them.

Fig. 21 Installation case 1

Fig. 22 Installation case 2

In addition, some flexible barriers caught debris at different sites. Fig.23 shows a supplemental case.

Fig. 23 Collapsed soil caught by the flexible barrier

The design values and the verification values of the capture results are compared by analyzing the mode of slope failure and the condition of barrier deformation as follows:

Table 5 Comparison of Design values and capture results

Item	Design value	Verification value of capture results
Maximum earth pressure	19.8 kN/m^2	24.1 kN/m^2
Maximum impact force	135.9 kN/m^2	120.7 kN/m^2
Amount of debris caught	312 m^3	approx. 350 m^3

Although the amount of debris caught and the maximum earth pressure measured by the capture result turned out to be larger than used in the design, the maximum impact force was the opposite. However, the maximum impact force that determined the barrier structure turned out to be the value closer to the design value. Members did not suffer any major deformation or rupture causing structural problems to the barrier. Therefore, it is assumed that the functions almost as envisaged by the design have been materialized.

6. CONCLUSION

The process of development of the flexible barrier, including implementation of the full-scale test mentioned before, the results of debris capture by the flexible barriers, and the results of comparison between the retaining wall and flexible barrier by DEM-based simulation are summarized as follows:

(1) The flexible barrier exhibits structural performance capable of resisting the impact force caused by the collapsed soil, as calculated from the Notification Equation, within the predetermined range (up to maximum impact of 150 kN/m^2).
(2) The flexible barrier exhibits structural performance capable of resisting the earth pressure generated by the collapsed soil, as calculated from the Notification Equation, within the predetermined range (up to the maximum barrier height of 5.5 m).
(3) The barrier is capable of maintaining the predetermined catch capacity before and after its deformation as a result of the capture of collapsed soil.
(4) When a flexible barrier is designed based on the allowable stress design method, the post interval and barrier height can be set in various values depending on the conditions. The safety of this barrier has been proven by full-scale tests and debris capture results.
(5) Simulation conducted under the same conditions indicates that the impact force acting on the impact-receiving face is more mitigated by the flexible barrier than the retaining wall. When a retaining wall is opted for, its structural size has to be large, so as to ensure the required capture performance.
(6) According to the results of impact force calculation using the Notification Equation and the simulation results, the impact force tends to be smaller for the latter than the former under fixed conditions (slope gradient of 45° or under).

As explained above, the flexible barrier is capable of effectively absorbing impact by allowing deformation and is considered suitable for installation particularly in confined spaces or on steep terrain where installation of retaining walls is difficult.

The authors intend to accumulate more data on debris capture results and continue verification of the performance of the flexible barrier; to endeavor to verify impact mitigation factors in design; to improve cost-efficiency of the barrier by reducing the weight of its members; and to enhance maintenance performance.

When a flexible barrier is installed on unstable ground, it is necessary to further enhance the safety of the post foundation and anchorage that ultimately receive the load in order to maintain stable functionality over extended periods of time. That is one of the major tasks to be tackled in the future.

REFERENCES

SABO & Land slide Technical Center (2011): Report of Construction Technology Review and Certification for

Impact Barrier work, pp53-54
Japan Flexible Barrier Association(2013): Designing manual of Impact barrier, pp. 25.
JSECE(2004): Revised SABO Glossary, pp. 231.
Musashi, Y., Yamasaki, M., Mizuyama, T., Kosugi, K.(2011):Study on the simulation method of collapsed soil movement, Journal of the Japan Society of Erosion Control Engineering, Vol. 64, No. 3, pp. 37-45 (in Japanese with English abstract)
Notification of the Ministry of Land, Infrastructure, Transport and Tourism No. 332 (2001): Notification on the methods specified by the Minister of Land, Infrastructure, Transport and Tourism as per the provision of Item 2, Article 2, Enforcement Order for the Law related to Promotion of Measures for Sediment-related Disaster Area etc. due to Sediment-related Disaster
WSL(2008): LB, Test report of KTI-Hangmuren St.Leonard
WSL(2010): LB, AVB, CW, Test report of KTI-Hangmuren Feltheim